Available online at www.sciencedirect.com
ScienceDirect
Cement and Concrete Research 38 (2008) 422–426
Cement and Concrete Research

Influence of the C/S and C/A ratios of hydration products on the chloride ion binding capacity of lime-SF and lime-MK mixtures

H. Zibara [a], R.D. Hooton [b], M.D.A. Thomas [c], K. Stanish [d,*]

[a] Department of Civil Engineering, McMaster University, 1280 Main St W., Hamilton, Ontario, Canada L8S 4L7
[b] Department of Civil Engineering, University of Toronto, 35 St. George St, Toronto, Ontario, Canada M5S 1A4
[c] Department of Civil Engineering, University of New Brunswick, 17 Dineen Dr., PO Box 4400, Fredericton, New Brunswick, Canada E3B 5A3
[d] Walker Restoration Consultants, 505 Davis Rd., Elgin, Il, 60123, USA

Received 31 October 2006; accepted 23 August 2007

Abstract

The mechanisms of chloride ion binding in cementitious systems when supplementary cementing materials are present are not completely understood, although it is believed to relate to the alumina content of the mixture. This relationship is investigated through the use of lime–silica fume and lime–metakaolin mixtures. It was found that while the alumina content does have an important influence, the chloride binding capacity was also controlled by the calcium-to-alumina and calcium-to-silica ratios. At a high C/A ratio, the formation of monocarboaluminate is favoured, which has a high ability to form Friedel's salt, and does so at low chloride concentrations (less than 0.1 M). With a low C/A ratio, the formation of stratlingite is favoured, with little formation of monocarboaluminate. If alumina is not present, chloride is bound by the C–S–H phase. The binding capacity of the C–S–H was found to depend on its calcium-to-silica ratio, C–S–H with a higher C/S having a greater binding capacity.

Keywords: Hydration products (B); Chloride (D); Blended cement (D); X-ray diffraction (B)

1. Introduction

The ability of concrete to bind chloride ions and retard their rate of penetration is an important factor in determining the service life of concrete structures with regards to chloride-induced corrosion. As such it has been extensively studied, and some of its mechanisms are beginning to be understood. For plain Portland cement mixtures, the primary mechanism is the formation of Friedel's salt and related complexes from the aluminate phases [1–7], although there is evidence that C–S–H can bind chloride ions as well [3,8–11]. However, its contribution is normally considered secondary.

In blends of Portland cement and supplementary cementitious materials (SCM), the influence of the SCM on chloride binding is believed to be a function of the aluminate content. While this has generally proven to be the case [12–14], there is some evidence to the contrary [15]. More importantly, however, the effect of inclusion of SCM's is more significant than that which would be expected solely from the change in alumina content [16]. Nilsson et al. [17] suggested that the partial replacement of cement with silica fume will have three main effects which will influence the binding capacity: 1) a reduction in the pH of the pore solution which will increase chloride binding, 2) a dilution of C_3A which will reduce binding, and 3) an increase in the amount of the C–S–H which should increase binding. It is also known that this replacement results in the formation of C–S–H with lower C/S than the C–S–H formed without the presence of silica fume [18]. It is not likely that the dilution of the C_3A can solely explain the observed reduction in the binding capacity as a result of the partial replacement of cement with silica fume.

To isolate the effect of silica fume and metakaolin, a series of experiments were conducted using lime mixtures. Lime was used rather than portland cement so as to isolate the binding mechanisms that occur with the hydrated silica fume or

* Corresponding author.
E-mail address: kyle.stanish@walkerrestoration.com (K. Stanish).

0008-8846/$ - see front matter © 2007 Elsevier Ltd. All rights reserved.
doi:10.1016/j.cemconres.2007.08.024

metakaolin. The influence of SF and MK when mixed with Portland cement were investigated in a separate study reported elsewhere [19].

2. Experimental procedures

To investigate the effect of varying alumina and silica proportions, two supplementary cementing materials were used. Silica fume (SF) contains greater than 90% silica, but almost no alumina. Metakaolin (MK) contains both silica and alumina in approximately equal proportions. The oxide compositions of the silica fume and metakaolin used are shown in Table 1. Mixtures of SF–lime and MK–lime were tested for their chloride binding capacity. Three different SCM/lime proportions were used — 2/1 (SF21), 1/1 (SF11), and 1/2 (SF12) by mass. Since up to 30% SF replacement is needed to react with all the $Ca(OH)_2$ produced as a result of hydration, a 2/1 ratio of SF to lime was an upper limit in the amount of SCM that could be included. A greater proportion of silica fume would result in unreacted particles. The SCM/lime ratios were then varied so that the resulting C–S–H hydrates would have different C/S ratios. A w/cm ratio of 2.0 was chosen to obtain workable mixes without the addition of a superplasticiser. The mix water contained 85 mmol/L NaOH and 345 mmol/L KOH to simulate alkali concentrations previously determined in a control, 100% Portland cement mixture [19]. The mixes were cured for 2 months at 38 °C to accelerate the pozzolanic reactions prior to testing.

The equilibrium procedure proposed by Tang and Nilsson [9] to establish chloride binding isotherms of cement pastes was followed in this work. At the end of the curing period, the pastes were demolded and the central portion was saw-cut into approximately 3-mm thick discs using a wet diamond blade lubricated with distilled water. The sliced samples were vacuum dried for three days in a desiccator containing silica gel and soda lime. They were then stored for a month in a glove box kept at 11% RH (using saturated lithium chloride solution). Soda lime was used to remove the carbon dioxide from the air inside the glove box. It has been reported that only a monolayer of water remains on the surface of cement hydrates at 11% RH [20], and this has been assumed to apply to the SF–lime and MK–lime hydrates studied here. After storage, 25 g samples were stored in 125 ml plastic bottles and placed under vacuum for about two hours. The bottles were filled with a known volume (approximately 60 mL) of NaCl solutions of varying concentrations (0.1, 0.3, 0.5, 0.7, 1.0, 2.0, 3.0 M Cl). The chloride solutions were saturated with calcium hydroxide (3 g/L, pH = 12.5) to prevent the leaching of calcium hydroxide from the samples during storage. The bottles were sealed and stored in the open laboratory atmosphere (22 °C), for 5–6 weeks to allow equilibrium to be established by diffusion of the chloride ions into the paste samples. This period of time was selected based upon experience with similar mixtures in identical experimental conditions. After equilibrium between the pore solution of the samples and the host solutions was reached, the host solutions were analyzed for chloride concentration, after appropriate dilution, by means of potentiometric titration with a Metrohm DMS760 automatic titrator versus 0.01 molar $AgNO_3$ titrant with a silver electrode.

Table 1
Oxide compositions of silica fume and metakaolin (mass %)

	SiO_2	Al_2O_3	TiO_2	P_2O_5	Fe_2O_3	CaO	SrO
Silica fume	94.48	0.24	0.01	0.14	0.63	0.44	0.02
Metakaolin	52.01	44.72	1.6	0.09	0.58	0.00	0.02
	MgO	Mn_2O_3	Na_2O_3	K_2O	$(Na_2O)_{eq}$	SO_3	LOI
Silica fume	0.38	0.03	0.16	1.01	0.82	0.36	2.87
Metakaolin	0.00	0.01	0.32	0.19	0.45	0.12	0.9

It is assumed that after equilibrium is reached between the external solution and the pore solution of the sample, the reduction in the concentration of the host solution is due solely to chloride being bound by the cement. Then, knowing the initial and final concentration, the volume of the external solution and the dry mass of the sample, the amount of bound chloride can be calculated according to the following formula:

$$C_b = 35.453V(C_i - C_e)/W_d \quad (1)$$

Where:

C_b amount of bound chloride in mg Cl/g of sample.
V volume of the external solution in mL.
C_i initial chloride concentration of the external solution in mol/L,
C_e free chloride concentration at equilibrium of the external solution in mol/L.
W_d dry mass of the sample in g, and
35.453 is the molar mass of the chloride ion.

The W_d mass is calculated using the formula:

$$W_d = W_{11}(1 - \zeta_{11}) \quad (2)$$

Where:

W_{11} mass of the sample at 11% RH in g,
ζ_{11} evaporable water content at 11% RH.

The free chloride ion concentrations were then plotted versus the bound values for each mixture to obtain the isotherms.

After equilibrium had been established, samples for XRD testing were taken out of the chloride solutions and wiped with a dry cloth to removes excess solution. They were then vacuum dried for three days in a dessicator containing silica gel and soda lime. After drying, the samples were removed to a low (11%) relative humidity environment that contained soda lime (to absorb the CO_2 in the air) where they were ground to powder and sealed in vials. The vials were returned to the dessicator to await testing. The X-ray diffraction patterns were obtained on a Siemens D5000 X-ray diffractometer using filtered CuKα radiation with a wavelength $\lambda = 15.418$ nm.

3. Results and discussion

3.1. Silica fume–lime mixtures

The XRD results (Fig. 1) showed the formation of C–S–H as the main hydration product in the SF12 and SF21 pastes. It can thus be assumed that C–S–H was the main hydration product in the SF11 paste as well. The XRD pattern of a sample of the SF21 paste revealed that all $Ca(OH)_2$ was consumed in the reaction with silica fume, as shown in Fig. 1. A semi-quantitative XRD analysis (estimating relative quantities by comparison of peak intensities) showed that the SF12 sample was 20% $Ca(OH)_2$ by mass after hydration, as compared to 66% of the original composition. This means that approximately 70% of the original $Ca(OH)_2$ had reacted with silica fume. Assuming that the silica fume was completely consumed, the average C/S ratios in the C–S–H of the SF21 and SF12 pastes would be 0.42 and 1.24 respectively. For the SF21 paste, this assumption results in the calculated C/S ratio (0.42) being unrealistically low. Values of C/S ratio as low as 0.65 were reported in low lime C–S–H in silica fume–lime mixtures dispersed in water (water/solid=200) [21], but this should be considered a lower limit. Thus for the SF21 paste, their likely remains unreacted silica fume. While the C/S ratio in the SF21 paste might not be 0.42, it is most likely lower than the C/S ratio in the SF12 paste. In addition, the amount of C–S–H in the SF21 paste would be higher than those in the SF12 paste due to the complete consumption of lime.

The influence of different C/S ratios can be seen in Fig. 2, showing the binding isotherms of the three SF–lime mixtures. While the SF12 (silica fume/lime=1/2) paste exhibited a capacity to bind chloride, the SF11 (silica fume/lime=1/1) exhibited a very small binding capacity, and the SF21 (silica fume/lime=2/1) paste had no binding capacity. The XRD pattern of the SF21 paste indicated that all the $Ca(OH)_2$ reacted with the silica fume, and thus formed the greatest amount of C–S–H. Yet this paste had no binding capacity. This indicates that the observed differences in the chloride binding capacities of the SF–lime pastes are not due to differences in the amounts of the C–S–H in the different pastes. They might instead be attributed to the possible differences in the properties of the C–S–H

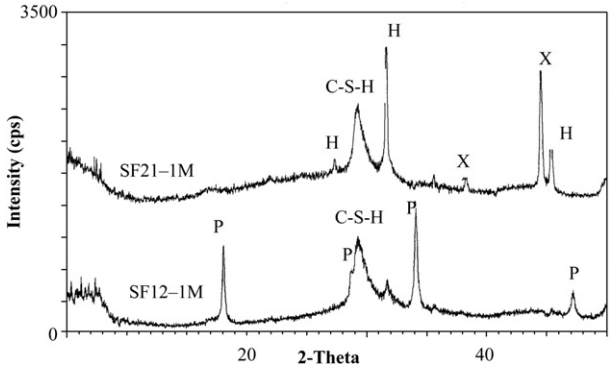

Fig. 1. XRD patterns of samples of the SF12 and SF21 paste that were exposed to 1 M chloride solution. P: Portlandite, H: halite(NaCl), X: sample holder reflection.

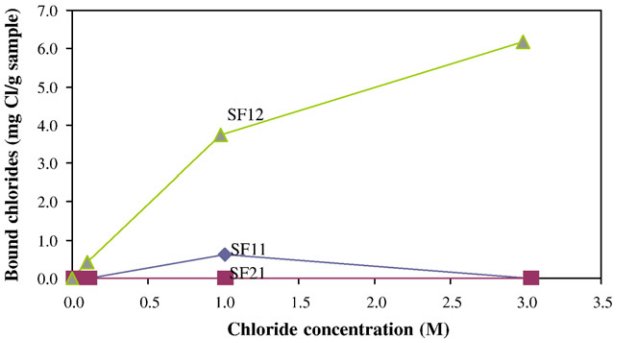

Fig. 2. Chloride binding isotherms of the SF–lime pastes.

formed in the different pastes. The differences in the chloride binding capacities of the C–S–H might be related to the differences in their C/S ratio: the higher the C/S ratio of the C–S–H, the higher the binding capacity of the C–S–H. This has been suggested by other workers (e.g. Glass et al. [22]). Therefore, it is possible that despite the increase in the amount of the C–S–H as a result of the partial replacement with silica fume, the net effect would be a decrease in the amount of bound chloride by the C–S–H due to lowering of the C/S ratio.

3.2. Metakaolin–lime mixtures

The metakaolin chemical composition is about 52% SiO_2 and about 45% AlO_3 and the products of hydration of the MK–lime mixtures are C–S–H, C–A–S–H, and C–A–H. Due to presence of both silica and alumina in MK, the C/S ratio of the C–S–H would be expected to be greater than for the C–S–H produced by the reaction of SF with lime discussed above. It is not possible to calculate an estimated C/S ratio due to the greater number of reaction products than contained in the SF–lime mixture. It is therefore expected both that the calcium aluminate hydrates and the C–S–H would contribute to the binding capacity. This is confirmed by the binding isotherms of the three MK–lime pastes as shown in Fig. 3. The MK–lime pastes have a much larger binding capacity compared to their equivalent SF–lime pastes.

Differences in binding capacity between different MK–lime mixtures cannot be attributed to differences in available alumina, however. The metakaolin mixtures exhibited a decrease in binding capacity with increasing metakaolin content, and thus increase alumina content. The binding capacities were larger the

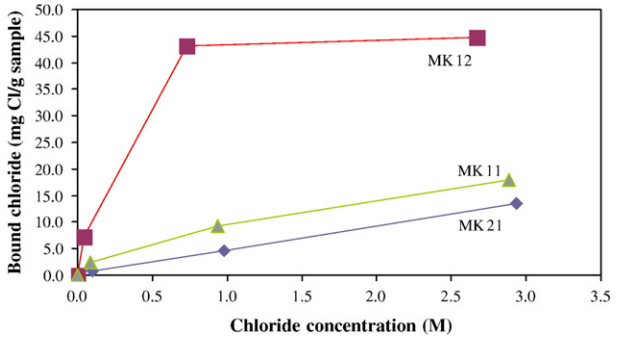

Fig. 3. Chloride Binding Isotherms for the MK–lime pastes.

lower the mass ratio of metakaolin to $Ca(OH)_2$ (MK/$Ca(OH)_2$) of the pastes. The MK12 (metakaolin/lime = 1/2) paste, which had the lowest MK/$Ca(OH)_2$ ratio, exhibited the highest chloride binding capacity and the MK21 (metakaolin/lime = 2/1) paste, which had the highest MK/$Ca(OH)_2$ ratio exhibited the lowest binding capacity.

An explanation for these observations can be seen from examination of the XRD patterns shown in Figs. 4 and 5. Fig. 4 shows the XRD patterns of samples of the MK12 paste exposed to 0 M, 0.1 M, 1.0 M, and 3.0 M NaCl while Fig. 5 shows the XRD patterns of the MK21 paste, but only at 0.1 and 3.0 M NaCl concentrations. For the MK12 paste, several hydration products were identified in the pastes not exposed to chlorides. They included portlandite, stratlingite, C–S–H, $Ca_3Al_2(SiO_4)(OH)_8$ and $Ca_3AlFe(SiO_4)(OH)_8$. In addition to these compounds, the largest intensity peak was identified as corresponding to the AFm compound, $C_3A{\cdot}CaCO_3{\cdot}11H_2O$, known as monocarboaluminate. This phase is known to occur as a hydration product in pozzolan–lime mixtures [19]. The hydration products of the MK21 paste, as seen in the 0.1 M exposure condition of Fig. 5, were different than those of the MK12 paste. The main compounds present were those of stratlingite and C–S–H. Beside the stratlingite, there were no clear signs of other AFm compounds or calcium aluminate hydrates or of portlandite. This difference in the hydration products between the MK12 and the MK21 pastes is related to the mass ratio of metakaolin to $Ca(OH)_2$.

Upon exposure to chloride solutions, both pastes produced Friedel's salt. However, due to the presence of monocarboaluminate, more Friedel's salt was formed in the MK12 mixture at lower chloride concentrations. The XRD results for the MK12 mixture indicated complete transformation of the monocarboaluminate to Friedel's salt upon exposure to a 0.1 M NaCl solution. For paste MK21, there is little Friedel's salt formed on exposure to a 0.1 M NaCl solution, and what little is formed is due to the transformation of stratlingite. Upon exposure to higher concentration chloride solutions, there is an increase in Friedel's salt production for both mixtures apparently due to transformation of stratlingite. However, stratlingite is still present at the highest chloride concentrations.

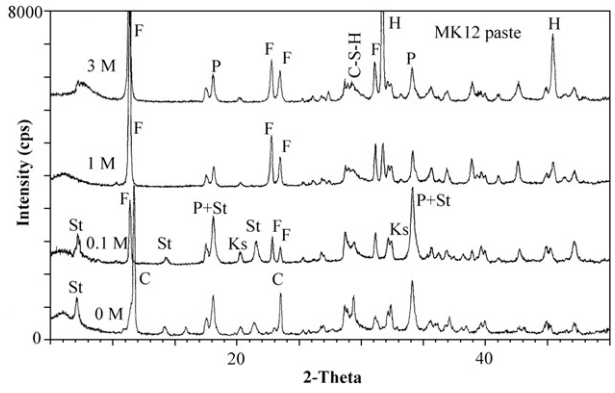

Fig. 4. XRD Patterns of Samples of the MK12 pastes that were exposed to different chloride concentrations. C: Monocarboaluminate, F: Friedel's salt, H: NaCl, Ks: kaolinite, P: portlandite, St: stratlingite.

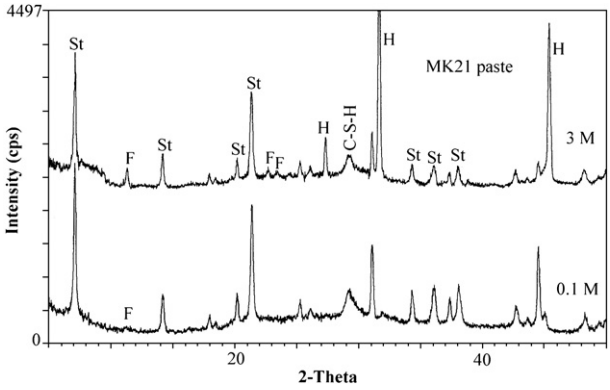

Fig. 5. XRD Patterns of Samples of the MK21 pastes that were exposed to different chloride concentrations, F: Friedel's salt, H: NaCl, St: stratlingite.

The amounts of Friedel's salt formed correspond with the binding isotherm results — a large increase in binding between 0 and 0.1 M for the MK12 mixture that does not occur in the MK21 mixture, with gradual increases in bound chloride concentration with increasing solution concentration thereafter. These results point to the possibility that chemical binding, through the formation of Friedel's salt, is mostly responsible for the binding capacity of the metakaolin–lime pastes.

The persistence of stratlingite at high chloride contents would have an influence on chloride ion binding capacity of cement–silica fume blends. In this case, it is expected that C–A–S–H such as stratlingite would form as product of hydration of the calcium aluminate with the silica from the silica fume. Since the previous results indicate that stratlingite, and presumably other forms of C–A–S–H such as the kaolinite in the metakaolin mixtures, tend to persist at higher chloride concentrations without fully transforming into Friedel's salt, it is suggested that the expected reduction in the chemical binding capacity is not only due to dilution of the C_3A content (and C_4AF content), but it is also possibly due to the formation of additional C–A–S–H when silica fume is added. With the blending of silica fume with a cement, not only is there proportionally less aluminate, more of it is in a form which has a low ability to bind chloride ions.

4. Discussion

Tests on cement–silica fume blend (8% replacement level), using the same silica fume used in the SF/lime mixtures, indicate a reduction in the chloride binding capacity of the blend [19]. The XRD results also show a reduction in the chemical binding capacity of the blend evidenced by the reduction in the Freidel's salt peaks [19]. However, no additional testing was performed to show the formation of stratlingite as a hydration product in the cement–silica fume paste [19]. Some studies showed the reduction in Friedel's salt content as a result of partial replacement of cement with silica fume[23,24]. However, the authors are unaware of any research that associated the presence of stratlingite in the hydrated cement–silica fume paste and the reduction in chloride binding capacity of the same paste.

5. Conclusions

Using silica fume–lime and metakaolin–lime mixtures, the role of different cementitious hydrates in chloride ion binding has been studied. When alumina is present, the primary mechanism of chloride ion binding is the formation of Friedel's salt. Depending upon the C/A ratio, however, different hydrates are formed which have a different binding capacity. At a high C/A ratio, the formation of monocarboaluminate is favoured, which has a high ability to form Friedel's salt, and does so at low chloride concentrations (less than 0.1 M). With a low C/A ratio, the formation of stratlingite is favoured, with little formation of monocarboaluminate. Stratlingite does convert to Freidel's salt, but at a much lower rate and much of the stratlingite persists at higher chloride concentrations.

If alumina is not present, the role of C–S–H in binding is revealed. Its binding capacity, while significantly less than that of the aluminate phases, can still be significant, due to the relatively large volumes of C–S–H in concrete. It was found to depend upon the C/S ratio, with a higher C/S ratio promoting greater chloride ion binding.

Acknowledgements

The authors would like to acknowledge the assistance of Dr. S. Petrov, Department of Chemistry, University of Toronto, with the X-ray diffraction testing.

The first author would like to acknowledge the financial support from Materials and Manufacturing Ontario during this project.

References

[1] M.H. Roberts, Effect of calcium chloride on the durability of pre-tensioned wire in prestressed concrete, Magazine of Concrete Research 14 (42) (1962) 143–154.
[2] P.K. Mehta, Effect of cement composition on corrosion of reinforcing steel in concrete, in: D.E. Tonini, S.W. Dean Jr. (Eds.), Chloride Corrosion of Steel in Concrete, ASTM STP, vol. 629, 1977, pp. 12–19.
[3] S. Diamond, Chloride concentrations in concrete pore solutions resulting from calcium and sodium chloride admixtures, Cement, Concrete and Aggregates 8 (2) (1986) 97–102.
[4] H.F.W. Taylor, Cement Chemistry, 2nd Edition, Academic Press Ltd., London, 1992 475 p.
[5] Rasheeduzzafar, Influence of cement composition on concrete durability, ACI Materials Journal 89 (6) (1992) 574–585.
[6] A.M. Neville, Chloride attack of reinforced concrete: an overview, Materials and Structures 28 (1995) 63–70.
[7] A.K. Suryavanshi, J.D. Scantlebury, S.B. Lyon, Mechanisms of Friedel's salt formation in cements rich in tri-calcium aluminate, Cement and Concrete Research 26 (5) (1996) 717–727.
[8] G. Blunk, P. Gunkel, H.-G. Smolcyzk, On the distribution of chloride between the hardening cement paste and its pore solution, 8th International Conference on the Chemistry of Cement, 1986, pp. 85–90.
[9] L. Tang, L.-O. Nilsson, Chloride binding capacity and binding isotherms of OPC pastes and mortars, Cement and Concrete Research 23 (2) (1993) 247–253.
[10] O. Wowra, M.J. Setzer, Sorption of chlorides on hydrated cement pastes and C3S pastes, in: M.J. Setzer, R. Auberg (Eds.), Frost Resistance of Concrete, E & FN Spon, London, 1997, pp. 147–153.
[11] C.K. Larsen, 1998, Chloride binding in concrete — effect of surrounding environment and concrete composition, Ph.D. Thesis, The Norwegian University of Science and Technology, Norway.
[12] N. Kouloumbi, G. Batis, C.h. Malami, The anticorrossive effect of fly ash, slag and a Greek pozzolan in reinforced concrete, Cement and Concrete Composites 16 (1994) 253–260.
[13] U. Weins, P. Scheissl, Chloride binding of cement paste containing fly ash, in: H. Justnes (Ed.), Proceedings of the 10th International Conference on the Chemistry of Cement, vol. 4, 1997, paper 4iv016, 10 pp., Gothenburg, Sweden.
[14] R.K. Dhir, M.A.K. El-Mohr, T.D. Dyer, Developing chloride resisting using PFA, Cement and Concrete Research 27 (11) (1997) 1633–1639.
[15] S.E. Hussain, Rasheduzzafar, Corrosion resistance performance of fly ash blended cement concrete, ACI Materials Journal 91 (3) (1994) 264–272.
[16] J.J. Beaudoin, V.S. Ramachandran, R.F. Feldman, Interaction of chloride and C–S–H, Cement and Concrete Research 20 (6) (1990) 875–883.
[17] L.-O. Nilsson, E. Poulson, P. Sandberg, H.E. Sorensen, O. Klinghoffer, in: J.M. Fredriksen (Ed.), HETEK: Chloride Penetration into Concrete, State-of-the-Art, Transport Processes, Corrosion Initiation, Test Methods and Prediction Models, Report, vol. 53, The Road Directorate, Denmark, 1996, 151 pp.
[18] F. Massazza, Pozzolana and pozzolanic cements, Lea's Chemistry of Cement and Concrete, 4th ed., Arnold Publishers, London, 1998, p. 546.
[19] H. Zibara, Binding of External Chlorides by Cement Pastes, Ph.D. Thesis, Department of Civil Engineering, University of Toronto, 2001.
[20] V.S. Ramachadran, R.F. Feldman, J.J. Beaudoin, Concrete Science, Heyden & Sons Ltd., London, 1981, p. 19.
[21] M. Grutzeck, A. Benesi, B. Fanning, Silicon-29: magic angle spinning nuclear magnetic resonance study of calcium silicate hydrates, Journal of the American Ceramic Society 6 (72) (1989) 665–668.
[22] G.K. Glass, N.M. Hassanein, N.R. Buenfeld, Neural network modelling of chloride binding, Magazine of Concrete Research 49 (181) (1997) 323–335.
[23] C.L. Page, O. Vennesland, Pore solution composition and chloride binding capacity of silica fume cement pastes, Material and Construction 16 (19) (1983) 19–25.
[24] Rasheeduzzafar, S. Ehtesham Hussain, A.S. Al-Gahtani, Pore solution composition and reinforcement corrosion characteristics of microsilica blended cement concrete, Cement and Concrete Research 21 (6) (1991) 1035–1047.